Calcif Tissue Int (1984) 36:361–369

Calcified Tissue International

Compositional, Structural, and Phase Changes in *in vitro* Laser-Irradiated Human Tooth Enamel

S. Kuroda[1] and B. O. Fowler[2]

[1]Division of Inorganic Materials, Institute for Medical and Dental Engineering, Tokyo Medical and Dental University, Tokyo, Japan; and [2]Mineralized Tissue Research Branch, National Institute of Dental Research, National Institutes of Health, Bethesda, Maryland 20205, USA

Summary. Tooth enamel laser irradiated under certain conditions previously has been shown to have reduced subsurface demineralization rates. Identification of these laser-induced changes has bearing on understanding the dissolution rate reduction mechanism; some of these changes, ones that occur in high temperature regions, were studied in this report. X-ray diffraction and infrared spectroscopy were used to identify changes in enamel of extracted intact human teeth subjected to high energy density (~10,000 J/cm^2) 10.6 μm wavelength carbon dioxide laser irradiance. The laser irradiance melted the enamel apatite; this solidified melt was composed of minor phases of α-tricalcium phosphate, α-$Ca_3(PO_4)_2$, and tetracalcium phosphate, $Ca_4(PO_4)_2O$, and a major phase of modified apatite. The apatite modifications, as compared with the original were (1) reductions in contents of water, protein, carbonate, and chloride (or chloride rearrangement); (2) essentially no change in apatite hydroxide content; (3) possible incorporation of oxide replacing some hydroxide ions; and (4) an uptake of traces of carbon dioxide and cyanate. An infrared band at 434 cm^{-1} that appears in spectra of hydroxyapatite partially dehydroxylated by thermal treatment was assigned to oxide translation. This band was utilized to search for oxide formation in the laser-irradiated tooth enamel.

Key words: Laser-irradiated enamel — Apatite modifications — α-Tricalcium phosphate — Tetracalcium phosphate — Oxyhydroxyapatite.

Invention of the laser appears to be one of the epoch-making events in this century, and remarkable advances in laser technology are being made. The first laser applications to dentistry were reported by Stern and Sognnaes [1], Goldman et al. [2], and Schulte [3], and further investigations related to possible dental applications have been summarized [4, 5].

Intact tooth enamel surfaces laser irradiated at low energy densities (~10–50 J/cm^2) are known to have reduced subsurface acid demineralization rates as compared with unirradiated controls [6–10]; consequently, the potential use of lasers to reduce caries is apparent. The mechanisms and/or changes causing the reduced demineralization appear uncertain. Stern et al. [6] and Yamamoto and Sato [10] attributed the decrease in subsurface demineralization rates to reduced permeability whereas Borggreven et al. [11] suggested that chemical changes may be responsible.

A laser-irradiated tooth enamel surface will have a temperature gradient that decreases in temperature from the irradiated point of impingement; changes in the tooth enamel along this temperature gradient are expected to be different. High energy density laser irradiant conditions cause visually observable melting of tooth enamel. Even under low energy density irradiant conditions (~25–120 J/cm^2, 10.6 μm wavelength), slight surface melting has been detected [4, 12] which indicates very high temperature at the tooth enamel surface. Identification of the overall changes and changes along this temperature gradient in tooth enamel has bearing on understanding the acid dissolution rate reduction mechanism. Changes in the higher temperature gradient region effected by using high energy density laser irradiance were investigated in the present report.

Kantola et al. [13] demonstrated by X-ray dif-

Send offprint requests to B. O. Fowler at the above address.

fraction and Kuroda and Nakahara [14] by electron microscopy that CO_2 laser irradiance (10.6 μm wavelength) could produce recrystallization and growth of crystallite size in the apatite crystals of tooth enamel. In addition, CO_2 laser irradiantly-induced phase changes in tooth enamel from apatite to α-tricalcium phosphate (α-TCP), α-$Ca_3(PO_4)_2$, have been reported [13, 15]. Although the possibility of phase changes has been expected, no additional studies have been reported to find new compounds or compositional and structural changes in tooth enamel subjected to high energy density laser irradiance. Therefore, the present study was undertaken to further analyze for changes in laser-irradiated human tooth enamel by means of X-ray diffraction and infrared (IR) spectroscopy.

Materials and Methods

Extracted sound human incisors were removed from storage in alcohol, air dried at 23°C, and then laser irradiated. The labial surfaces of about 45 of these intact teeth, initially at room temperature, were irradiated with the incident nonpulsed laser beam perpendicular to the tooth. The teeth were irradiated at an energy density of ~10,000 J/cm^2 in the focused 10.6 μm wavelength beam from a CO_2 laser (Yoshida Mgf. Co., Inc., Japan). The original laser beam diameter of 4 mm was reduced by means of a lens to a spot diameter of about 0.5 mm at the tooth surface; the irradiation time was 1 sec and the laser output power was 20 W. A crater was produced in the tooth enamel at the irradiated site. The entire crater material (solidified meltedlike material) was removed, ground into a powder, and analyzed by X-ray diffraction and IR spectroscopy.

The synthetic calcium phosphate standards were prepared from reagent grade chemicals as follows: β-tricalcium phosphate (β-TCP), β-$Ca_3(PO_4)_2$, was prepared by heating a 1 to 1 molar mixture of $Ca_2P_2O_7$ and $CaCO_3$ at 1,000°C in air for 88 h; a portion of the β-TCP was heated at 1,200°C in air for 22 h to form α-TCP which was rapidly cooled to minimize conversion to β-TCP; tetracalcium phosphate (TETCP), $Ca_4(PO_4)_2O$, was prepared by heating a 1 to 2 molar mixture of $Ca_2P_2O_7$ and $CaCO_3$ at 1,200°C in vacuum for 22 h and then cooling under vacuum to exclude water vapor and prevent formation of hydroxyapatite (HA), $Ca_{10}(PO_4)_6(OH)_2$; and HA was prepared according to the procedure of Fowler [16]. The $Ca_2P_2O_7$ for the above preparations was prepared by heating $CaHPO_4$ at 1,000°C in air for 24 h. All reaction mixtures were mixed and ground in an acetone slurry to <10 μm particle size in a mechanical mixer-grinder, dried, and then pressed into pellets to ensure better solid-state reactions. The identities of all the above standards were verified by X-ray diffraction and IR spectroscopy. A portion of the above thermally-prepared anhydrous carbonate-free HA was partially dehydroxylated by heating at 800°C in vacuum (0.05 Torr) for 20 h and then cooling under the same pressure to 25°C. This vacuum-heat treatment caused 0.37 wt % loss (1.79 wt % loss is calculated for $Ca_{10}(PO_4)_6(OH)_2$ conversion to $Ca_{10}(PO_4)_6O + H_2O$). Samples having greater degrees of dehydroxylation were prepared as above, except higher temperatures (900–1,000°C) were used. The hydroxide reduction was evident from decreased intensities and areas of the apatite hydroxide bands in IR spectra.

Scanning electron microscopy was carried out using an Alpha-9 (Akashi Inc., Tokyo, Japan) scanning electron microscope operated at 15 kV. X-ray diffraction patterns of the powders were obtained in the 5–70° 2θ range with Cu K-alpha radiation using a JEOL JDX-8P X-ray diffractometer operating at 40 kV and 17.5 mA. Infrared percent transmittance and linear absorbance spectra of the ground samples (≤5 μm particle size) in 400 mg KBr pellets 13 mm in diameter were obtained in the 4,000 to 300 cm^{-1} region using a Perkin-Elmer Model 621 spectrophotometer purged with dry air. Blank KBr pellets were placed in the instrument reference beam to cancel sample beam absorptions arising from the KBr matrix. Apatite hydroxide contents of the normal and the laser-irradiated tooth enamel (with approximate corrections for additional phases) were estimated by the IR method of Fowler et al. [17] using band area ratios; relative changes in contents of other constituents were estimated from changes in their band areas normalized to the area of the apatite phosphate bands between 615 and 500 cm^{-1} or by equivalent sample weight comparisons. The laser-irradiated tooth enamel sample after irradiance was not always maintained in a dry atmosphere and some of the water evident in its IR spectra was probably picked up from the atmosphere.

Results

An SEM overview of the crater produced in tooth enamel by laser irradiance is shown in Figure 1; a cross-sectional view of the crater and higher magnification of the crater material are shown in Figures 2 and 3, respectively. The crater and its surface had the smooth and rounded appearance of a solidified melt (Figures 1 and 2), and some recrystallization was evident from the platelike and long slender crystals observed near the bottom edge of the crater side (Figure 3).

The X-ray diffraction powder pattern of the laser-irradiated tooth enamel, overall, agreed with that of HA. However, additional weak nonapatitic lines were observed at 3.88, 2.90, 2.80, 2.77, 2.71, and 2.62 Å, and many other weak lines were visible. The additional weak lines at 3.88, 2.90, and 2.62 Å correspond to major lines of α-TCP; the other lines, at 2.80, 2.77, and 2.71 Å, correspond to several major lines of TETCP.

Infrared percent transmittance spectra of normal unirradiated tooth enamel (NTE), laser-irradiated tooth enamel (LTE), HA, TETCP, and β- and α-TCP and higher sample concentration linear absorbance spectra of normal and laser-irradiated tooth enamel in the 4,000 to 300 cm^{-1} range are shown in Figure 4. The origins of the IR absorption bands for HA and most of those for tooth enamel in the above range have been reported (see [18] for HA in

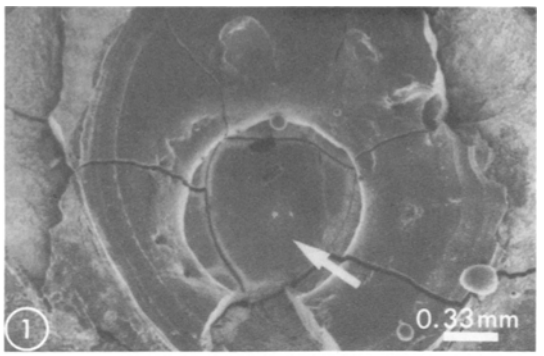

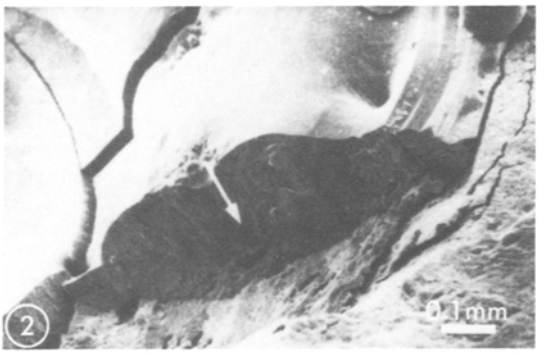

Fig. 1. SEM overview of crater produced in enamel surface of intact human tooth by carbon dioxide laser irradiance at an energy density of ~10,000 J/cm^2. ×24; bar = 0.33 mm.

Fig. 2. Cross-sectional view of side of crater shown in Fig. 1 at higher magnification. ×80; bar = 0.1 mm.

Fig. 3. Higher magnification of material in region indicated by *arrow* in Figure 2 showing platelike and long slender crystals. ×8,000; bar = 1 μm.

the 4,000–200 cm^{-1} range and [19] for tooth enamel in the 4,000–about 800 cm^{-1} range). The tooth enamel bands at 602 and 568 cm^{-1} (doublet) are well known to arise from the ν_4 phosphate mode. The tooth enamel band at 470 cm^{-1} arises from the ν_2 phosphate mode and the shoulder at about 350 cm^{-1} arises from hydroxide "translation" by comparison with the assigned modes in HA [18]. The spectra of the laser-irradiated tooth enamel show (1) a minor phase of TETCP by new bands of weak intensity at 502, 440, 400, and the very weak shoulders at ~985 and ~940 cm^{-1}; and (2) the major phase is still apatite (apatite phosphate bands at ~1090, ~1040, 958, 602, 568, and 470 cm^{-1}) but was modified. The percent reductions in constituents given below are based on the composite substance (all phases included) in the laser-irradiated tooth enamel as compared with the original constituent contents in the normal single phase tooth enamel apatite. Thus, the actual percent reductions in the separate modified apatite phase in the laser-irradiated tooth enamel are less; this will be considered in the discussion. The apatite phase was modified by (a) reduction in water content (broad band with maximum at ~3,350 cm^{-1} and 1,640 cm^{-1} band), (b) protein loss (2924 and 2854 cm^{-1} bands), (c) introduction of traces of molecular carbon dioxide (new very weak band at 2,340 cm^{-1} [19]) and cyanate, NCO^- (new extremely weak band at 2,200 cm^{-1} weakly evident in higher sample concentration absorbance spectrum [20]) from decomposed carbonate and/or protein, (d) about 66% reduction in carbonate content (1,546, ~1,465, 1,455, 1,412, 878, and 872 cm^{-1} bands), (e) a probable reduction in chloride content or change in chloride positions along the apatite hexad axis (about 70% reduction in area of 3,496 cm^{-1} band evident in 3,700 to 3,400 cm^{-1} inset due to OH---Cl interaction [21]), and (f) about 30% reduction in apatite hydroxide content (3570 cm^{-1} band).

The ratio of the 3,570 cm^{-1} hydroxide band area to the 602 plus 568 cm^{-1} ν_4 phosphate band areas in the 615 to 500 cm^{-1} range obtained from linear absorbance specta (not shown) was used to estimate the change in apatite hydroxide content [17]. This method also showed that the apatite hydroxide contents of the laser-irradiated and the normal unirradiated tooth enamel were ~0.35 and ~0.5, respectively, that of the essentially fully-hydroxylated HA standard in Figure 4. This HA standard has 99% of the theoretical hydroxide content by gravimetric deduction [16] and 97 ± 5% by chemical analyses [22, Table III, Sample S-1]. The apatite hydroxide content of the laser-irradiated tooth enamel was obtained by the ratio method assuming that tooth enamel apatite and the additional phases of α-TCP and TETCP all have the same ν_4 phosphate band area absorption coefficients. The approximate relative band area absorption coefficients (area/mg phosphate) measured for portions of the ν_4 phosphate band in the 615 to 500 cm^{-1} region used for the ratio method for α-TCP and TETCP were about 5 and 21% less, respectively, than that of HA. However, calculation showed that 20 wt % of these additional phases (10 wt % of each) admixed with HA

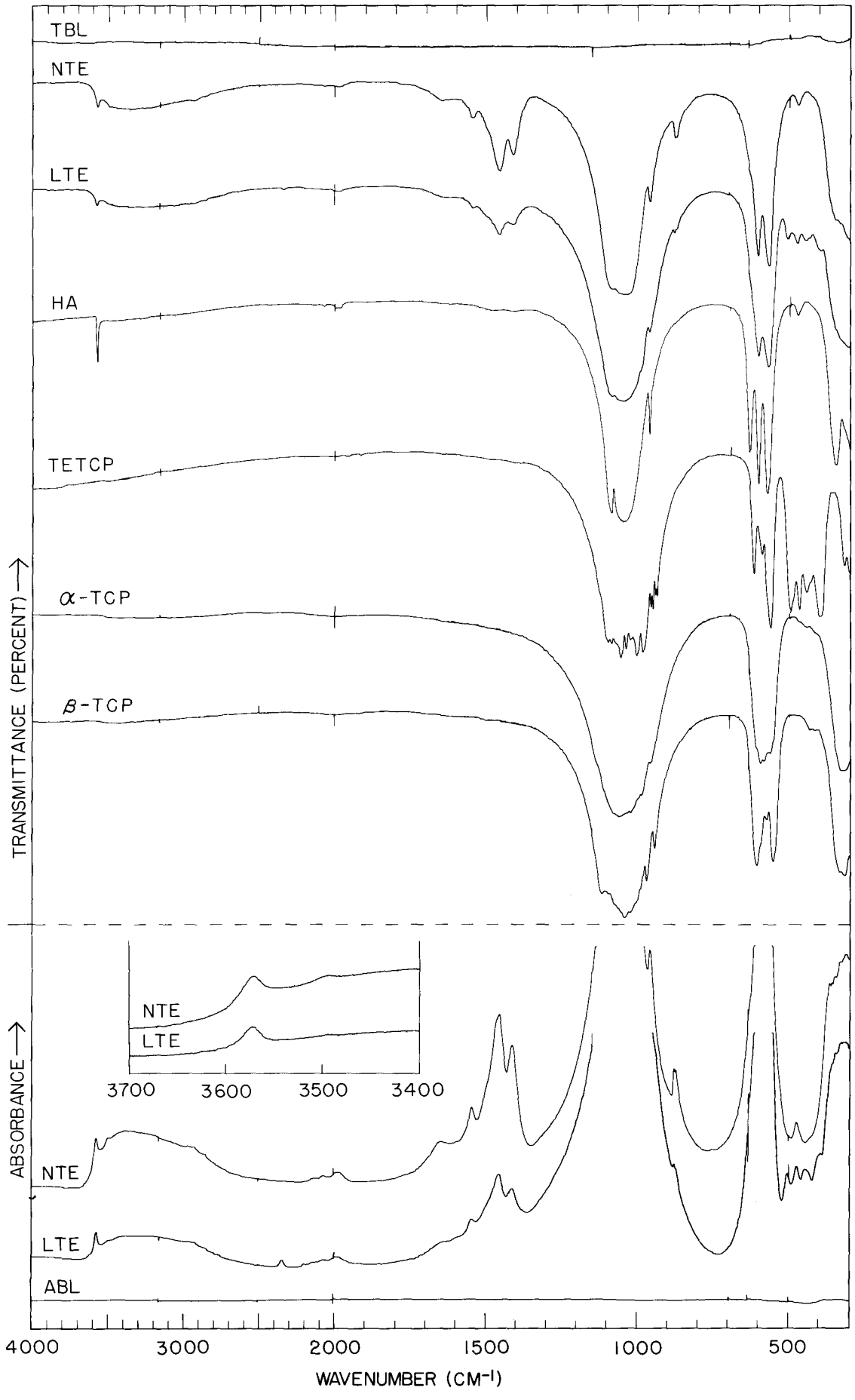
TBL
NTE
LTE
HA
TETCP
α-TCP
β-TCP
TRANSMITTANCE (PERCENT) ⟶
NTE
LTE
3700
3600
3500
3400
ABSORBANCE ⟶
NTE
LTE
ABL
4000
3000
2000
1500
1000
500
WAVENUMBER (CM⁻¹)

would cause an error of only +2.5% in the hydroxide determination. This small error introduced in hydroxide content, a few percent, was experimentally confirmed using a tooth enamel mixture containing ~10 wt % each of the additional phases. Consequently, the minor amounts of these additional phases in the laser-irradiated tooth enamel were expected to cause only a small error in the measured apatite hydroxide content. Also, the apatite hydroxide contents of the normal and the laser-irradiated tooth enamel estimated from 3,570 cm^{-1} hydroxide band areas per mg of sample were close to, but about 10% lower than, those estimated by the ratio method.

Infrared absorbance spectra of normal and the laser-irradiated tooth enamel, a mixture of normal tooth enamel containing ~10 wt % each of TETCP and α-TCP, the calcium phosphate standards, and a partially dehydroxylated HA are shown in Figure 5 in the 750 to 300 cm^{-1} region. Spectra of HA dehydroxylated by heating at 800–1,000°C in vacuum have two new principal bands in the 500–400 cm^{-1} region at ~475 and ~434 cm^{-1} whose intensities vary depending upon the degree of dehydroxylation. The dehydroxylation was estimated by weight loss and decreases in IR hydroxide band areas. The ~434 and ~475 cm^{-1} band areas predominate for dehydroxylation <~50 and >~50%, respectively; both bands shift slightly to higher wavenumbers with increasing dehydroxylation. The ν_2 phosphate bands also occur in this region (474 and ~462 cm^{-1} for HA) but have normal intensities much weaker than those observed for the ~434 and ~475 cm^{-1} bands. The spectrum of the partially dehydroxylated HA (~20% hydroxide loss inferred from the 0.37 wt % loss) in Figure 5 shows the new band at 434 cm^{-1} along with reduced hydroxide librational and translational band areas at 631 and ~350 cm^{-1}, respectively. The hydroxide translational band at ~350 cm^{-1} is composed of two bands at ~355 and 343 cm^{-1} [18]. The 434 cm^{-1} band is assigned to a $Ca_3^{2+}—O^{2-}$ vibrational mode (probably of the ν_3 type) where oxide (O^{2-}) has replaced hydroxide along the hexad axis based on the following (B. O. Fowler, unpublished results; see [18] for vibrational mode designations and [16] for isotopic apatite preparations):

(1) The 434 cm^{-1} band in spectra of partially dehydroxylated HA separately enriched with ^{18}O (~60% enrichment) and ^{48}Ca (97% enrichment) shifts ~15 and ~3 cm^{-1}, respectively, to lower wavenumbers which shows both oxygen and calcium motions occur in this mode.

(2) The band shift on ^{18}O enrichment could derive from a ν_2 phosphate mode (calculated ν_2 phosphate mode shift is ~ −15 cm^{-1} for 60% enrichment); however, the 434 cm^{-1} band develops intensity about three times that shown in Figure 5 and this is much greater than that expected by comparison to the weak ν_2 phosphate modes of HA, α-, and β-TCP that occur in the 475 to 400 cm^{-1} region in Figure 5.

(3) The possibility of the 434 cm^{-1} band arising from a ν_2 phosphate mode is further reduced because of the 434 cm^{-1} band shift on ^{48}Ca substitution; the internal phosphate vibrational modes of HA have previously been shown [16] to be very insensitive (≤1 cm^{-1} shifts) to calcium mass increase.

(4) The calculated wavenumber shifts for the 434 cm^{-1} band on (a) complete ^{18}O substitution is −25 cm^{-1} for independent oxide translation and ~ −22 cm^{-1} for the ν_3 and ν_2 modes of an isolated trigonal planar $Ca_3^{2+}—O^{2-}$ group and on (b) complete ^{48}Ca substitution, −4.3 cm^{-1} for the ν_2 mode of the $Ca_3^{2+}—O^{2-}$ group (ν_3 mode shift not calculated but expected to be ≥ −4.3 cm^{-1}). The 434 cm^{-1} band of the ~60% ^{18}O enriched apatite shifted ~ −15 cm^{-1}. This band appeared to shift as a whole, that is, two separate bands arising from possible localized $^{16}O^{2-}$ and $^{18}O^{2-}$ translational vibrations were not clearly resolved in spectra of the apatites at 48°C or at −185°C. This intermediate shift for the mixed $^{16,18}O^{2-}$ composition is consistent with that expected for a translatory lattice mode [23, 24].

(5) The higher wavenumber for the $Ca_3^{2+}—O^{2-}$ vibration, 434 cm^{-1} as compared with 343 cm^{-1} for the ν_3 type $Ca_3^{2+}—(OH)^-$ vibration, is consistent

Fig. 4. Infrared spectra of normal tooth enamel (*NTE*), laser-irradiated tooth enamel (*LTE*), hydroxyapatite (*HA*), tetracalcium phosphate (*TETCP*), and alpha and beta tricalcium phosphate (α-, β-*TCP*) in the 4,000–300 cm^{-1} range. Transmittance and linear absorbance spectra are shown at the top and bottom, respectively, along with the KBr transmittance base line (*TBL*) and the KBr absorbance base line (*ABL*). All spectra and base lines were run with a blank KBr pellet in the instrument reference beam. Sample concentrations, mg/400 mg KBr: transmittance spectra of *NTE* and *LTE* (1.10 mg each) and of calcium phosphate standards (0.80 mg each); absorbance spectra of *NTE* and *LTE* including 3,700–3,400 cm^{-1} expansion inset (all 4.0 mg). Both full range absorbance spectra are at A = 0.06 at 2,250 cm^{-1} and at A = 1.0 where the spectral lines end and continue (e.g., 1,140 and ~970 cm^{-1}). Spectral slit widths: ~6 cm^{-1} in range <3,000 cm^{-1} and >6 cm^{-1} in range >3,000 cm^{-1}.

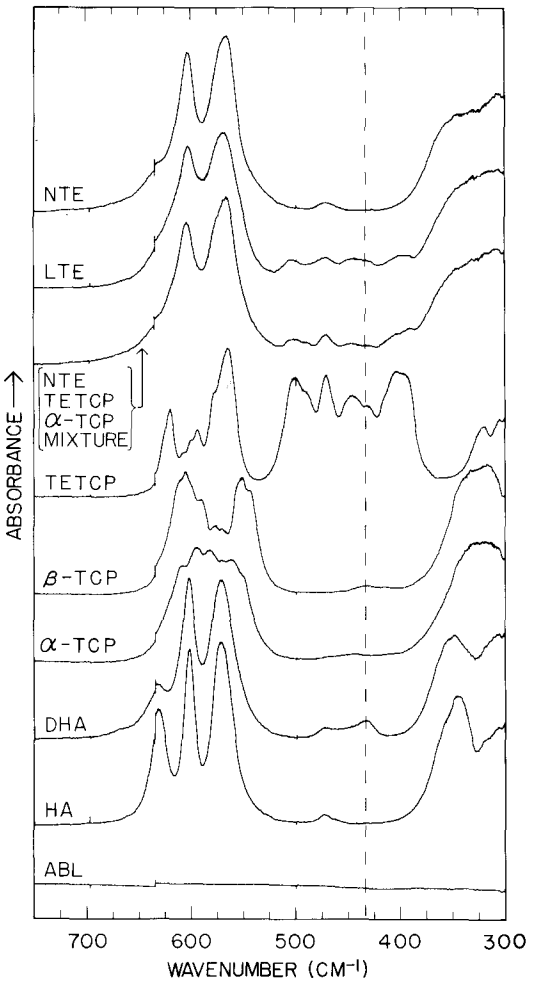

Fig. 5. Infrared absorbance spectra in the 750–300 cm^{-1} range. DHA denotes the spectrum of the partially dehydroxylated HA and the mixture contains ~10 wt % each of TETCP and α-TCP. Sample concentrations and recording conditions were the same as those for transmittance spectra in Figure 4 except the spectral slit width was ~3.5 cm^{-1}. The identifying letters have the same meanings as those in the Figure 4 legend.

with the expected stronger electrostatic bonding from O^{2-} in the Ca^{2+}—O^{2-} group and, to a slight extent, to the lighter mass of the oxide ion.

(6) The 434 cm^{-1} band intensity increases in intensity with concomitant decreases in the apatite hydroxide band intensities. No isotopic band shift measurements were carried out on the ~475 cm^{-1} band that predominates in intensity for dehydroxylation >~50%. However, because of the concomitant reduction in intensity of the 434 cm^{-1} band with an increase in intensity of the ~475 cm^{-1} band for dehydroxylation >~50% and expected increasing O^{2-} content, the ~475 cm^{-1} band also probably arises from vibration of Ca_3^{2+}—O^{2-} groups more strongly bonded than those causing the 434 cm^{-1} band.

Trombe and Montel [25, 26] have prepared and characterized calcium oxyapatite, $Ca_{10}(PO_4)_6O$. Their IR spectrum of a 75% dehydroxylated composition, $Ca_{10}(PO_4)_6O_{0.75}(OH)_{0.5}$, the most dehydroxylated degree they were able to stabilize after cooling under high vacuum to room temperature, shows a strong band (doublet) at ~475 cm^{-1} and two weak bands at ~440 and ~430 cm^{-1}. The strong band at ~475 cm^{-1}, as suggested above, probably arises from a Ca_3^{2+}—O^{2-} stretching mode and the weaker ones from ν_2 phosphate modes and/or a Ca_3^{2+}—O^{2-} mode of the weaker type.

The presence of oxide in partially dehydroxylated HAs has not been established by direct means. Hence, spectral comparison of the herein assigned oxide translational bands for oxyhydroxyapatite with oxide translational bands of a calcium phosphate having established oxide ions, for example, $Ca_4(PO_4)_2O$, is beneficial to help confirm the presence of oxide and the band assignments. Tetracalcium phosphate has two structurally discrete oxide ions, O(1) and O(2), and two each of O(1) and O(2) in its 4[$Ca_4(PO_4)_2O$] unit cell; each oxide ion is very strongly coordinated to four calcium ions that form approximate tetrahedrons about each oxide ion [27]. The IR spectrum of TETCP in Figure 5 in the 500–400 cm^{-1} region has four major bands and about four poorly resolved ones. These bands have apparently not been assigned. However, these major bands most probably derive from oxide translations, that is, vibrations of the Ca_4^{2+}—O^{2-} groups; many additional minor bands are also expected in this region from the ν_2 phosphate modes but poorly resolved because of the proximity of the major bands (B. O. Fowler, unpublished results). The wavenumber positions and number of oxide translational bands in spectra of $Ca_{16}(PO_4)_8O_4$ and $Ca_{10}(PO_4)_6(OH)_{2-x}O_{0.5x}$ are clearly expected to be different because of their structural differences; nonetheless, the oxide band positions for the two compounds are expected to occur in a similar wavenumber region. Consequently, the oxide vibrational assignment region, ~500–400 cm^{-1}, is mutually consistent for both compounds; this supports the assignment and presence of O^{2-} in the dehydroxylated HA.

The intensity of the ~440 cm^{-1} band in Figure 5 in the spectrum of the laser-irradiated tooth enamel that contains the minor second phases of TETCP and α-TCP is higher than that expected by comparison with the spectrum of the mixture of normal tooth enamel containing ~10 wt % each of TETCP and α-TCP. A second phase of β-TCP with its weak band at ~432 cm^{-1} would contribute to an increase in intensity of the ~440 cm^{-1} band; however, it would have to be present as a major phase to in-

crease the intensity to that observed. No β-TCP was detected in the laser-irradiated tooth enamel by X-ray diffraction which is a more sensitive method for detection of β-TCP than the IR method. Consequently, the additional weak absorption contribution in the 440 cm^{-1} region in the laser-irradiated tooth enamel spectrum appears to arise from sources other than TETCP and/or α- and β-TCP and it may arise from oxide translation.

Discussion

The X-ray and IR data lead to the conclusion that the high energy density laser irradiance caused (1) formation of additional minor phases of α-TCP and TETCP and (2) compositional and structural modifications in the major apatite phase. Brune [28] also reported that the major product formed in tooth enamel by 10.6 μm wavelength CO_2 laser irradiance at an energy density of 1,000–20,000 J/cm^2 was apatitic in structure by X-ray diffraction. Tetracalcium phosphate is an expected high temperature reaction product, but its presence in laser-irradiated tooth enamel has not previously been reported. The detection of α-TCP by X-ray diffraction confirms previous findings [13, 15]. The additional minor phase of α-TCP was not detected by IR spectroscopy; the α-TCP spectra (Figs. 4 and 5) do not have sharp bands displaced from those of HA, which makes its detection in HA difficult.

Both the melted appearance and the presence of α-TCP and TETCP in the laser-irradiated tooth enamel indicated temperature >1,400°C at the irradiated tooth enamel site by comparisons with the approximate m.p. of tooth enamel, the temperature of thermal disproportionation of HA, and the m.p. of the disproportionation products. Human tooth enamel melts above 1,280°C [29]; HA disproportionates into a mixture of α-TCP and TETCP on heating at about 1,450°C in air [30] and this mixture melts at about 1,600°C [31].

The IR analyses showed the following previously unreported compositional and structural changes in the laser-irradiated tooth enamel: (1) reductions in contents of water, protein, carbonate (~66% reduction), apatite hydroxide (~30% reduction), chloride bonded to hydroxide (~70% reduction) or chloride rearrangement; (2) possible formation of oxide; and (3) an uptake of traces of carbon dioxide and cyanate. These percent reductions in apatite constituents are based on the combined phases formed on laser irradiance including the modified apatite, TETCP, and α-TCP. Consequently, the percent change in constituents in the separate modified apatite phase as compared with the original single apatite phase of normal tooth enamel will depend on the amounts of the additional phases present. Part or all of the reductions in some constituents could result from the apatite disproportionation to form the additional phases of TETCP and α-TCP. Disproportionation of 30% of the original apatite corresponds to a loss, for example, of 30% of the original hydroxide ions. The weak X-ray diffraction intensities for TETCP and α-TCP suggested that these phases combined comprised less than 30 wt % of the laser-irradiated tooth enamel composite. In addition, IR spectra of mixtures of normal tooth enamel and TETCP indicated ~10 wt % of the latter based on the bands in the 500–400 cm^{-1} region. Thus, considering an upper range of 20–30 wt % for the combined additional phases of TETCP and α-TCP, the carbonate, chloride, and hydroxide contents of the modified apatite phase were reduced by ~59–53, ~62–57, and ~13–0%, respectively. Using these approximate corrections, the laser-irradiated tooth enamel apatite phase appears to have no more apatite hydroxide than the original that was estimated to contain ~0.5 that of stoichiometric HA.

Holcomb and Young [32] have quantitated, by means of IR spectroscopy, changes in various constituents of human tooth enamel caused by heating in the range 25 to about 1,000°C in a tube furnace. Their samples were heated for 24 h at each temperature in both dried and undried N_2 atmospheres and were cooled to room temperature in the same atmospheres. Their IR analyses showed that tooth enamel progressively heated from 100–1,000°C in undried N_2 had an apatite hydroxide increase ~1.8 times the original in the ~300–500°C range and an apatite hydroxide level ~1.4 times the original in the ~600–1,000°C range. The tooth enamel apatite hydroxide decrease at 600°C probably arises from pyrophosphate reacting with a portion of the apatite phase to form β-TCP. Since the apatite hydroxide content of the laser-irradiated tooth enamel apatite phase did not change significantly and still contained about 0.5 the apatite hydroxide content of stoichiometric HA, supplemental hexad anions are expected to be present to maintain the observed hexagonal structure. Therefore, the presence of oxide in the thermally modified apatite phase, as suggested by the IR spectra, is consistent as a complement to the low hydroxide content. Holcomb and Young [32] suggested that their tooth enamel samples ignited at the higher temperatures (but under conditions not causing disproportionation) were essentially oxyapatites. Their spectrum of tooth enamel heated at 800°C (Fig. 1A) shows the ~434 cm^{-1} band (probably oxide absorption) and

of intensity much too high to derive from a minor second phase of β-TCP.

The laser-induced thermal changes in hydroxide, chloride, carbonate, cyanate, and carbon dixoide observed by IR in this study roughly correspond, except for carbonate rearrangement, to those reported for tooth enamel heated in a furnace at ~700°C in a dry N_2 atmosphere or at 1,100°C or higher for corresponding changes in hydroxide and chloride if the N_2 atmosphere was not dry [32]. The changes in relative intensities of the carbonate bands deriving from carbonate in hexad positions (1,546, ~1,465, and 878 cm^{-1} bands [19]) and in "phosphate" positions (1,455, 1,412, and 872 cm^{-1} bands [32, and references therein]) for the normal and the laser-irradiated tooth enamel in Figure 4 suggest only a slight relative increase of carbonate in the hexad positions of the total residual carbonate in the laser-irradiated tooth enamel. The hexad position carbonate content normally increases substantially relative to the phosphate position carbonate content as the latter decreases on heating tooth enamel progressively from ~500–~1,000°C [32, 20]. The high energy density laser irradiance and rapid resultant heating effected the compositional and structural changes in tooth enamel in seconds; this very rapid heating may restrict diffusion mechanisms and reactions that favor carbonate incorporation in hexad positions. The presence of the minor phases of the high temperature, >1,400°C, products of α-TCP and TETCP and the major phase of modified apatite having constituent changes corresponding to the thermal product range of ~700–~1,100°C, dependent upon atmosphere, illustrate a considerable and expected temperature gradient at the laser-irradiated tooth enamel site.

No measurements were carried out to detect the decrease in acid phosphate (HPO_4^{2-}) content of the normal tooth enamel on laser irradiance; however, no acid phosphate was expected in the laser-irradiated substance because of the high temperatures. Acid phosphate in normal tooth enamel converts to pyrophosphate ($P_2O_7^{4-}$) between ~300 and 600°C [33, 34]; the pyrophosphate formed reacts at higher temperature, ~650–700°C, with a portion of the apatite phase to form β-TCP [33].

The additional phases of α-TCP and TETCP formed under the high energy density laser irradiance conditions (~10,000 J/cm^2, 10.6 μm wavelength) used in this report are not expected to form to any large extent under the low energy density irradiance conditions (~10–50 J/cm^2, 10.6 μm wavelength) that reduced tooth enamel subsurface demineralization rates [7, 8]. However, these phases may be formed under low energy density conditions in thin layers at the tooth enamel surface as suggested by surface melting [4, and references therein; 12]; also, the compositional and structural changes herein reported are expected in (1) the major modified apatitic phase that is intermixed in the fused-melted layer and (2) to a decreasing extent for most changes in the adjacent unmelted layers. The probable effects of the additional phases of α-TCP, TETCP, and β-TCP expected to form at lower temperatures, and the herein reported and other compositional and structural changes in tooth enamel on its solubility will be given in a separate report (Fowler and Kuroda, in preparation).

References

1. Stern RH, Sognnaes RF (1964) Laser beam effect on dental hard tissues. J Dent Res 43 (Suppl. to No. 5):873, Abstract 307
2. Goldman L, Hornby P, Meyer R, Goldman B (1964) Impact of the laser on dental caries. Nature 4943:417
3. Schulte W (1964) Präparation der Zahnhartsubstanzen mit dem Laser-Strahl? Zahnärztl Mitt 54:892–894
4. Stern RH (1974) Dentistry and the laser. In: Wolbarsht ML (ed) Laser applications in medicine and biology, Vol. 2, Plenum Press, New York, pp 361–388
5. Stern RH, Eastgate H, Mautner WJ, Morgan C (1975) The laser in dentistry: potential clinical applications. Opt Laser Technol 7:22–24
6. Stern RH, Sognnaes RF, Goodman F (1966) Laser effect on in vitro enamel permeability and solubility. J Am Dent Ass 73:838–843
7. Stern RH, Vahl J, Sognnaes RF (1972) Lased enamel: ultrastructural observations of pulsed carbon dioxide laser effects. J Dent Res 51:455–460
8. Stern RH, Sognnaes RF (1972) Laser inhibition of dental caries suggested by first tests in vivo. J Am Dent Ass 85:1087–1090
9. Yamamoto H, Ooya K (1974) Potential of yttrium-aluminum-garnet laser in caries prevention. J Oral Path 3:7–15
10. Yamamoto H, Sato K (1980) Prevention of dental caries by Nd:YAG laser irradiation. J Dent Res 59:2171–2177
11. Borggreven JMPM, van Dijk JWE, Driessens FCM (1980) Effect of laser irradiation on the permeability of bovine dental enamel. Arch Oral Biol 25:831–832
12. Boehm R, Rich J, Webster J, Janke S (1977) Thermal stress effects and surface cracking associated with laser use on human teeth. J Biomech Eng 99:189–194
13. Kantola S, Laine E, Tarna T (1973) Laser-induced effects on tooth structure. VI. X-ray diffraction study of dental enamel exposed to a CO_2 laser. Acta Odont Scand 31:369–379
14. Kuroda S, Nakahara H (1981) Morphological changes in laser-irradiated extracted teeth. J Dent Res 60 (Special Issue A): Abstract 719
15. Lobene RR, Bhussry BR, Fine S (1968) Interaction of carbon dioxide laser radiation with enamel and dentin. J Dent Res 47:311–317
16. Fowler BO (1974) Infrared studies of apatites. II. Prepara-

tion of normal and isotopically substituted calcium, strontium, and barium hydroxyapatites and spectra-structure-composition correlations. Inorg Chem 13:194–207
17. Fowler BO, Hailer AW, Meyer JL (1980) Infrared and Raman studies of hydroxide quantitation in apatitic calcium phosphates. J Dent Res 59 (Special Issue A): Abstract 391
18. Fowler BO (1974) Infrared studies of apaptides. I. Vibrational assignments for calcium, strontium, and barium hydroxyapatites utilizing isotopic substitution. Inorg Chem 13:194–207
19. Elliott JC (1974) The crystallographic structure of dental enamel and related apatides. PhD Thesis, University of London
20. Dowker SEP (1980) Infrared spectroscopic studies of thermally-treated carbonate-containing apatites. PhD Thesis, University of London
21. Dykes E, Elliott JC (1971) The occurrence of chloride ions in the apatite lattice of Holly Springs hydroxyapatite and dental enamel. Calcif Tissue Res 7:241–248
22. Meyer JL, Fowler BO (1982) Lattice defects in nonstoichiometric calcium hydroxylapatites. A chemical approach. Inorg Chem 21:3029–3035
23. Matossi F (1951) Interpretation of the vibrational spectrum of mix-crystals. J Chem Phys 19:161–163
24. Snyder RG, Kumamoto J, Ibers JA (1960) Vibrational spectrum of crystalline potassium hydroxide. J Chem Phys 33:1171–1177
25. Trombe JC, Montel G (1978) Some features of the incorporation of oxygen in different oxidation states in the apatitic lattice-I. J Inorg Nucl CHem 40:15–21
26. Trombe JC, Montel G (1978) Some features of the incorporation of oxygen in different oxidation states in the apatitic lattice-II. J Inorg Nucl Chem 40:23–26
27. Dickens B, Brown WE, Kruger GH, Stewart JM (1973) $Ca_4(PO_4)_2O$, Tetracalcium diphosphate monoxide. Crystal structure and relationships to $Ca_5(PO_4)_3OH$ and $K_3Na(SO_4)_2$. Acta Cryst B29:2046–2056
28. Brune D (1980) Interaction of pulsed carbon dioxide laser beams with teeth in vitro. Scand J Dent Res 88:301–305
29. Corcia JT, Moody WE (1974) Thermal analysis of human dental enamel. J Dent Res 53:571–580
30. Newesely H (1977) High temperature behavior of hydroxy- and fluorapatite. J Oral Rehabil 4:97–104
31. Welch JH, Gutt W (1961) High-temperature studies of the system calcium oxide-phosphorus pentoxide. J Chem Soc 4442–4444
32. Holcomb DW, Young RA (1980) Thermal decomposition of human tooth enamel. Calcif Tissue Int 31:189–201
33. Herman H, Dallemagne MJ (1961) The main mineral constituent of bone and teeth. Arch Oral Biol 5:137–144
34. Arends J, Davidson CL (1975) HPO_4^{2-} content in enamel and artificial carious lesions. Calcif Tissue Res 18:65–79